



Arsenic Removal from Aqueous Solutions using Iron Oxide-modified Zeolite: Experimental and Modeling Investigations

L. Sanaei¹, M. Tahmasebpour^{1,*}, M. Khatamian², B. Divband^{3,4}

¹ Faculty of Chemical & Petroleum Engineering, University of Tabriz, Tabriz, Iran

² Physical Inorganic Chemistry Research Laboratory, Department of Inorganic Chemistry, Faculty of Chemistry, Tabriz, Iran

³ Dental and Periodontal Research Center, Tabriz University of Medical Sciences, Tabriz, Iran

⁴ Infectious and Tropical Diseases Research Center, Tabriz University of Medical Sciences, Tabriz, Iran

ABSTRACT: Arsenic in drinking water has been recognized as a serious community health problem because of its highly toxic nature and therefore, its removal is considered as one of the most important areas of wastewater treatment. Iron oxide-modified zeolite nanocomposites with two different amounts of iron oxide nanoparticles (3 & 7 wt%) were synthesized, characterized by X-ray diffraction, scanning electron microscope, energy dispersive X-ray, and Brunauer-Emmett-Teller, and then used in a series of batch adsorption experiments to remove arsenic from aqueous system. The effective parameters on the removal of arsenic including adsorbent dose, arsenic initial concentration, contact time, and percentage of iron oxide nanoparticles, were investigated. Under optimum conditions, percentage of iron oxide nanoparticles 3%, adsorbent dose 0.05 g/l, arsenic initial concentration 400 g/l, and contact time 90 min, the iron oxide-modified zeolite could remove up to 87% of arsenic from contaminated water. The artificial neural network model was also developed from batch experimental data sets which provided reasonable predictive performance ($R^2=0.998$) of arsenic adsorption. According to the results, iron oxide-modified zeolite appears to be a promising adsorbent for removing arsenic from water.

Review History:

Received: 14/10/2019

Revised: 20/12/2019

Accepted: 10/03/2020

Available Online: 12/03/2020

Keywords:

Arsenic

Fe₃O₄-NaA Zeolite

Water-treatment

Artificial Neural Network

1. INTRODUCTION

Arsenic (As(V)) is one of the contaminants found in the environment which affects millions of people and other living organisms across the world due to its high toxicity even at very small concentrations [1, 2]. Arsenic in groundwater is largely due to the minerals dissolving naturally from weathered rocks and soils when water is exposed to these natural components. Furthermore, it has many industrial applications and is also used extensively in the production of agricultural pesticides and treated wood products, which all may introduce arsenic into the environment [3, 4]. Long-term exposure to arsenic-contaminated drinking water can develop into arsenicosis which causes respiratory, renal, and immunologic effects [5]. It also can cause cancer of the skin, lungs, bladder, kidney, liver, and prostate [6, 7]. As a result, the World Health Organization (WHO) has set the arsenic standard for drinking water to a level less than 10g/l, since 1993 [8]. This maximum contaminant limit was also adopted in the United States (US) since 2006 [9].

Among different treatment methods applicable for arsenic-contaminated water; such as adsorption [2], coagulation/precipitation [4], lime softening [10], membrane process [11], and anion-exchange [12], adsorption has proven to be an efficient, low cost and more familiar method by the local population, suppliers and engineering companies [12]. Numerous sorbents; including

magnetite-reduced graphene oxide [13], magnetic gelatin-modified biochar [14], nanoscale zero-valent iron [15], iron-oxide coated coal bottom ash [16], Fe₃O₄ nanoparticles [17], chemically modified sawdust [18], aluminum hydroxide [19] and zeolites [2], have been tested in the literature for their arsenic removal abilities from aqueous solutions. However, the development of new materials for arsenic removal is still a hot topic in the environmental field. In recent years, a wide range of materials have been used to modify the surface of sorbents and then to develop more efficient arsenic adsorbents. It has been reported that arsenic anions present in water have a strong adsorption affinity to iron oxides/hydroxides [20] and accordingly, adsorbents modified with iron are increasingly applied for the removal of arsenic [21-24].

Zeolites are a group of 3D crystalline alumina-silicates which have many advantages because of their specific structure like high adsorption and ion-exchange capabilities and also relatively low cost [5]. They are classified according to the differences in their framework structure, Si to Al ratio, pore size, hydrophilicity, etc, which are critical factors in determining their properties [25]. Different kinds of zeolites; namely clinoptilolite [20], A [26], and Y [27], have been identified as potential candidates for arsenic removal from water. Among them, single-phase zeolite NaA has been of great interest because of its large cation exchange capacity and a large number of acid sites due to its 8-ring, 6-ring, and

*Corresponding author's email: tahmasebpour@tabrizu.ac.ir



4-ring channel structure with the largest cavity dimension measuring $0.41 \text{ nm} \times 0.41 \text{ nm}$ [28].

The main purpose of this study was to develop NaA zeolite modified with iron oxide (Fe_3O_4) nanoparticles and to investigate the application of Fe_3O_4 -NaA nanocomposites for the removal of As(V) from contaminated water. Fe_3O_4 nanoparticles were selected as modification agents due to their high surface area, high active sites on the surface, being easily separated, collected, and reused by an external magnetic field, and also being environmentally friendly [29, 30]. The influence of different sorption parameters including adsorbent dose, As(V) initial concentration, percentage of Fe_3O_4 nanoparticles, and contact time on the removal of As(V) were studied experimentally. Besides, the adsorption experiments were statistically modeled using Artificial Neural Network (ANN) to predict the removal efficiency of Fe_3O_4 -NaA nanocomposites for As(V) ions. The most important novelty of current research is synthesizing Fe_3O_4 -NaA nanocomposite by quick precipitation method in just one step reaction under mild conditions. Besides, the ANN modeling seems applicable to estimate the arsenic removal efficiency from water by Fe_3O_4 -NaA nanocomposite.

2. MATERIAL AND METHODS

2.1. Materials

All chemicals were of analytical grade, purchased from Merck Co., and used without further purification. A stock solution of As(V) was prepared by dissolving sodium arsenate hydrate ($\text{Na}_2\text{HAsO}_4 \cdot 7\text{H}_2\text{O}$) in distilled water and it was used to prepare the sorbate solutions with concentrations of 50, 150, 400, and 1000 $\mu\text{g/l}$. This is the common range of arsenic groundwater contamination in Southeast Asia. Reaction vessels were cleaned with 1% HNO_3 and rinsed several times with distilled water before use.

2.2. Preparation Of Nano Fe_3O_4 -Naa Zeolite

Firstly, 5.24 g Al_2O_3 and 5 g sodium silicate were added to 90 ml NaOH (1.73 M) solution. This solution was stirred for 10 h and then ultrasounded for 90 min before 20 ml Fe_3O_4 suspension was added during the ultrasound. After the formation of amorphous homogenous gel, the reaction mixture was transferred into a steel autoclave vessel and heated for 8 h at 80°C without stirring. The sediment of nanocomposites at the bottom of the vessel was filtered, washed with deionized water thoroughly, and dried at 120°C overnight. By changing the amount of nano Fe_3O_4 , NaA zeolites with various nano iron oxide contents (3 & 7 wt%) were prepared and designed as IO_nNaA ($n = 3 \& 7$).

2.3. Characterization Of Materials

X-Ray Diffraction (XRD) measurements were employed for the identification of phases of the synthesized Fe_3O_4 -NaA zeolite using a Philips X-ray diffractometer model D5000 siemens (Cu $K\alpha$, $\lambda = 1.5416 \text{ \AA}$). The intensity data were collected over a 2θ range of $4-70^\circ$ with a step of 0.05 and a scanning rate of 2 s/point. The surface images of synthesized zeolites were taken by Scanning Electron Microscope

(SEM) (model ESEM XL 30 Philips) operating at 30 kV and equipped with Energy Dispersive X-ray (EDX) analysis to investigate the morphology, size, and elemental analysis of the nanocomposites. As(V) determination was performed using Varian 220 electrothermal atomic absorption spectroscopy. The Brunauer-Emmett-Teller (BET) surface area was also measured by N_2 adsorption/desorption isothermal liquid nitrogen using Quantachrom (chembet 3000).

2.4. Batch Experiments

Sorption experiments were performed in a batch system to examine the effect of different parameters including adsorbent dose, As(V) initial concentration, percentage of Fe_3O_4 nanoparticles, and contact time on the removal of As(V). 100 mL aqueous solution of arsenic was taken in an Erlenmeyer flask of volume 250 mL at 25°C . The pH value was adjusted to 7, generally representative of the typical pH of natural water. Then, a known quantity of dried Fe_3O_4 -NaA zeolite adsorbent was added and the arsenic bearing suspension was kept under magnetic stirring until various intervals of time. After the complete sorption, the suspension was allowed to settle down, Fe_3O_4 -NaA zeolite composites were separated by filter and the filtered solution was analyzed for As(V). The percentage removal of arsenic from aqueous solution was computed by using the following equation:

$$\text{Percentage removal of arsenic} = \frac{C_i - C_f}{C_i} \times 100 \quad (1)$$

where C_i and C_f are the initial and final arsenic concentrations in the solution, respectively.

2.5. Ann Modeling

The application of ANN has been successfully employed in environmental engineering to predict the performance of wastewater treatment processes [31-33]. In the present research, the single-subject experimental datasets obtained from the batch experiments were used as inputs to the ANN model to provide the reasonable predictive performance of the Fe_3O_4 -NaA zeolite adsorbent. The backpropagation algorithm is the most versatile and robust technique, which provides the most efficient learning procedure for MultiLayer Perception (MLP) networks [34]. A feed-forward MLP network was employed with Levenberg-Marquardt backpropagation algorithm to build the predictive ANN mathematical model with the scaled condition of the four inputs (e.g., As(V) initial concentration, contact time, adsorbent dose, and percentage of Fe_3O_4 nanoparticles) and one output as As(V) removal efficiency. The neural network topology consisted of three layers: an input layer, a hidden layer, and an output layer. Out of 35 datasets, 80% (=27 groups) experiments were used to train the network, and the remaining 20% (=8 groups) were used for testing and validation of the ANN model. All input and output data were normalized between 0 and 1 to avoid numerical overflows due to large or small values. Therefore, data (X_i) are converted into a normalized value (X_{normal}) as follows [35]:

$$X_{normal} = \frac{(X_i - X_{min})}{(X_{max} - X_{min})} \quad (2)$$

where X_{min} and X_{max} are minimum and maximum actual experimental data, respectively.

All calculations carried out using Matlab R2015b (8.6.0.267246) mathematical software with ANN toolbox.

3. RESULTS AND DISCUSSION

3.1. Characterization

The positions and intensities of the peaks in the XRD diffraction pattern are a fingerprint of the crystalline components present in a sample. The XRD patterns of the synthesized NaA zeolite and IO₃NaA and IO₇NaA nanocomposites are presented in Fig. 1. These samples contain various percentages of Fe₃O₄ nanoparticles as 0, 3, and 7%, respectively. For neat zeolite NaA (Fig. 1(A)), sharp peaks are seen in the diffractogram; indicating its high crystallinity. The characteristic reflections for zeolite NaA were appeared at $2\theta=7.24^\circ$, 10.14° , 12.41° , 16.04° , 21.93° , 24.20° , 26.89° , 27.37° , 28.13° , 30.20° , 31.51° , 33.03° and 34.25° which are in good agreement with the data of crystalline form of zeolite NaA given in relevant literature [28, 36, 37]. The absence of the peaks related to impurities as well as the absence of amorphous halo region in the XRD pattern of the zeolite NaA indicates that highly pure and crystalline zeolite has been synthesized. In addition, the XRD patterns of the synthesized IO_nNaA nanocomposites (Figs. 1(B,C)) did not show any notable change in NaA-zeolite diffraction peaks except that the intensity of reflections was slightly decreased. This suggested that obvious damage in cell structures of NaA zeolites did not take place, and the magnetic particles could be found within the XRD features of the synthesized NaA-zeolite. The diffraction peaks at 18.27° , 30.20° , 34.25° , 42.27° , 52.96° , 54.82° , and 63.17° are attributed to the existence of Fe₃O₄ in the zeolitic network. It might be expected that the loaded nanoparticles are preferentially precipitated on the surface of zeolite without any considerable change in the microporous of NaA-zeolites.

The morphology and size of the zeolites are of determining factors for their performance in any specific application. The SEM observations of the IO_nNaA nanocomposites synthesized under various Fe₃O₄ contents are shown in Figs. 2(A,B). The figures confirm the crystalline nature of nanocomposites, which can be described in terms of small cubic particles with an average size of approximately 300-600 nm. The cubic structure of the nanocomposites shows that the NaA zeolite structure; which has been reported as cubic in the literature [36, 38-41], has not changed by the formation of Fe₃O₄ as expected by the results of XRD analyses. The Fe₃O₄ nanoparticles which are irregular and spherical-like particles are seen as favorably dispersed on the external crystal surface of IO₃NaA without any considerable agglomeration (Fig. 2(A)). By increasing the iron oxide content to 7%, aggregation of Fe₃O₄ nanoparticles are obviously identified between the NaA nanozeolites (Fig. 2(B)). In agreement, the

BET specific surface area for NaA zeolite and IO₃NaA and IO₇NaA nanocomposites are determined to be 17.03, 65.5, and 53.3 m²/g, respectively.

The elements present in the IO_nNaA nanocomposites are characterized with the help of EDX analysis, which is shown in Fig. 2(C). This elemental analysis reveals that the main chemical compositions of the synthesized magnetic zeolite include Na, Al, Si, Fe and O. The appeared peak in the region of 6.5 keV is related to the binding energy of Fe, which indicates the presence of iron in the product. The Au peak is observed due to the gold coating of the sample.

3.2. Batch Adsorption Study

Results on the adsorption of As(V) by IO_nNaA zeolites at different conditions and pH=7 are presented as a percentage of arsenic removal in Figs. 3(A,B). The As(V) initial concentrations of 50, 150, 400, and 1000 g/l, adsorbent dose of 0.01 and 0.05 g/l, contact time of 60 and 90 min, and Fe₃O₄ nanoparticles percentage of 3 and 7% were employed in batch studies. Since the predominant forms of As(V) in water with pH=7 are anionic forms of H₂AsO₄⁻ and HAsO₄²⁻, so, iron oxides which are mainly present with the cationic monomeric form [Fe(OH)₂]⁺ in this pH, can adsorb As(V) more easily, because of Coulombic interactions [8]. Also, the normal range for pH in surface water systems is 6.5 to 8.5, and the pH range for groundwater systems is between 6 to 8.5, then we decided to choose pH=7 for all the experiments.

As seen in the figures, arsenic removal curves show apparent changes as IO_nNaA zeolite dose rises from 0.01 to 0.05 g/l. The higher dose of adsorbent in the solution results in greater availability of exchangeable sites for the ions and that is the reason for increasing arsenic removal rate with increasing the amount of adsorbent. It seems that 0.01 g/l of IO_nNaA adsorbent is very low amount to reach a reasonable arsenic removal efficiency. So that, the percentage removal achieves the maximum level of approximately 20 and 35% in the presence of 0.01 g/l of adsorbent for an adsorption period of 60 and 90 min, respectively. Furthermore, changes in other parameters such as contact time or As(V) initial concentration, don't lead to certain behavior in arsenic removal efficiency due to the very low amount of adsorbent (0.01 g/l). However, it is observed that over 80% As(V) with initial concentration 400 g/l is adsorbed by the 0.05 g/l of adsorbent at 90 min exposure time. We found that 0.1 g of IO₃NaA adsorbent is sufficient to remove 400 µg As(V) from 11 aqueous solution to meet the standard value of arsenic disposal in wastewater, which was confirmed by determining As(V) concentration in the filtrate.

Experiments performed on 0.05 g/l of adsorbent showed that arsenic removal efficiency increases with an increase in arsenic concentration up to 400 g/l and then is fixed at higher concentrations. At low initial concentration, metal ions in the solution are also low and the possibility of interaction between ions and active sites on the adsorbent surface will be a significant factor in the sorption efficiency. When the As(V) initial concentration is increased, this possibility is also increased and more arsenic ions are adsorbed on

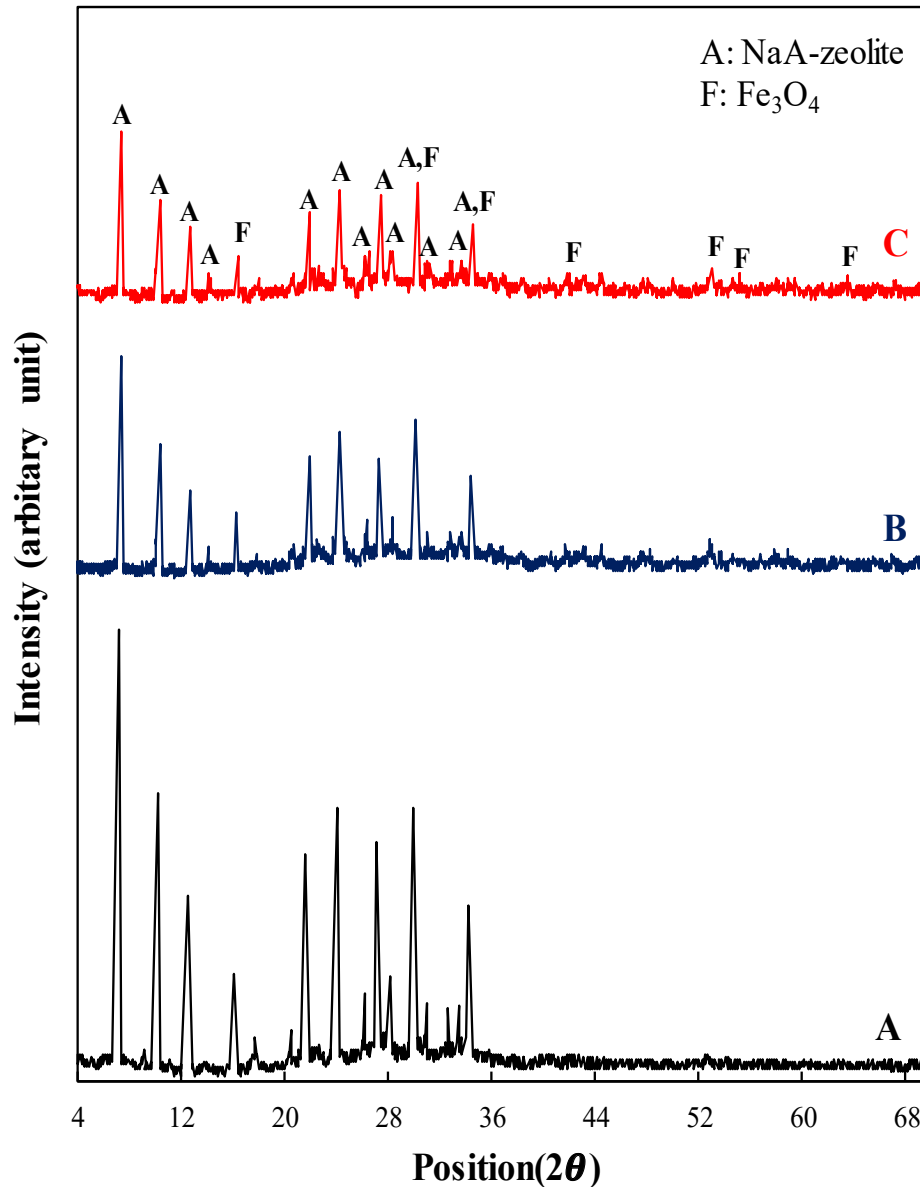


Fig. 1. XRD patterns of (A) synthesized NaA-zeolite and (B) IO₃NaA and (C) IO₇NaA nanocomposites

the surface of Fe₃O₄-NaA zeolite [42]. In other words, the high initial concentration enhances the driving force and thus in turn lowers the mass transfer resistance between the aqueous solution and the solid adsorbent [43]. When metal ion concentrations are more increased, binding sites become more quickly saturated as the amount of adsorbent concentration remained constant [33]. The large amount of adsorbed arsenic is proven to have an inhibitive effect on the adsorption of arsenic ions on the adsorbent, because of the lack of any direct contact between them. At a high enough initial concentration, the Fe₃O₄-NaA zeolite will be saturated with arsenic molecules and the number of active sites on the adsorbent surface will not be enough to accommodate arsenic ions.

One of the other parameters that affect the arsenic removal efficiency is the percentage of Fe₃O₄ nanoparticles loaded in NaA zeolite structure. The effect of this parameter on the removal of arsenic by IO_nNaA zeolite was investigated by varying the Fe₃O₄ loading. The results indicate that arsenic removal decreases slightly when Fe₃O₄ loading increases from 3 to 7%. It is proposed that the surface of IO_nNaA is covered by some Fe₃O₄ nanoparticles which probably block some zeolite cavities and the blockage area would increase with the higher amount of Fe₃O₄ loading. This is in agreement with the SEM pictures in which the aggregation of the iron oxide nanoparticles occurred on the surface of sample IO₇NaA with higher iron oxide content. In the case of sample IO₃NaA, the homogenous dispersion of nanoparticles allows

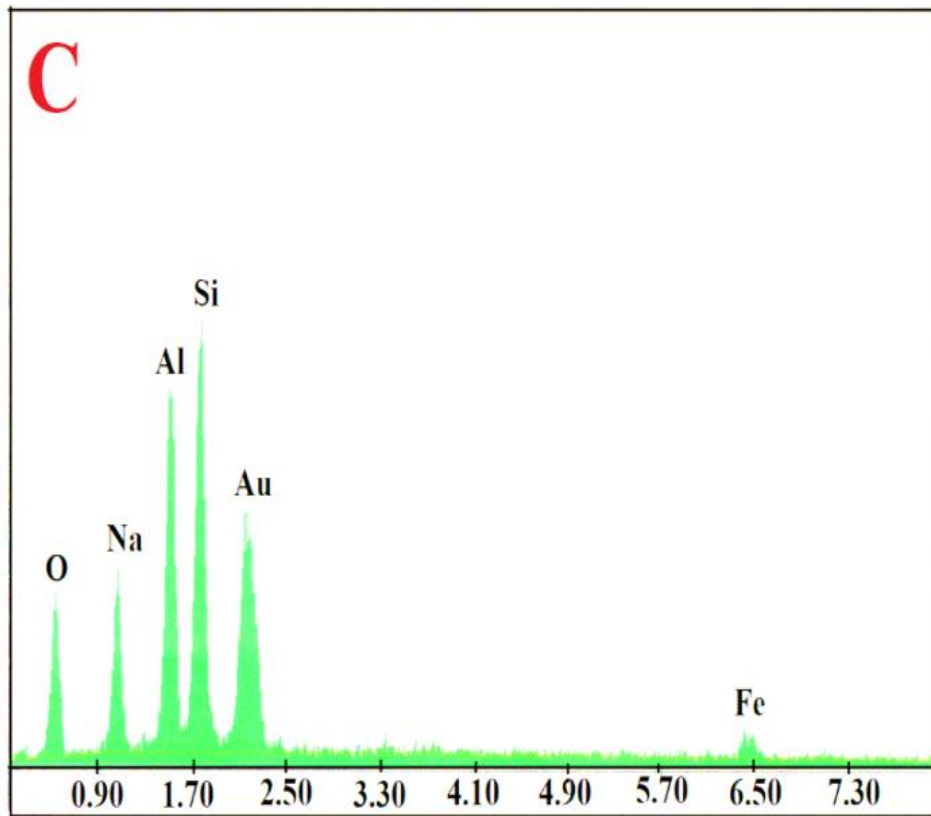
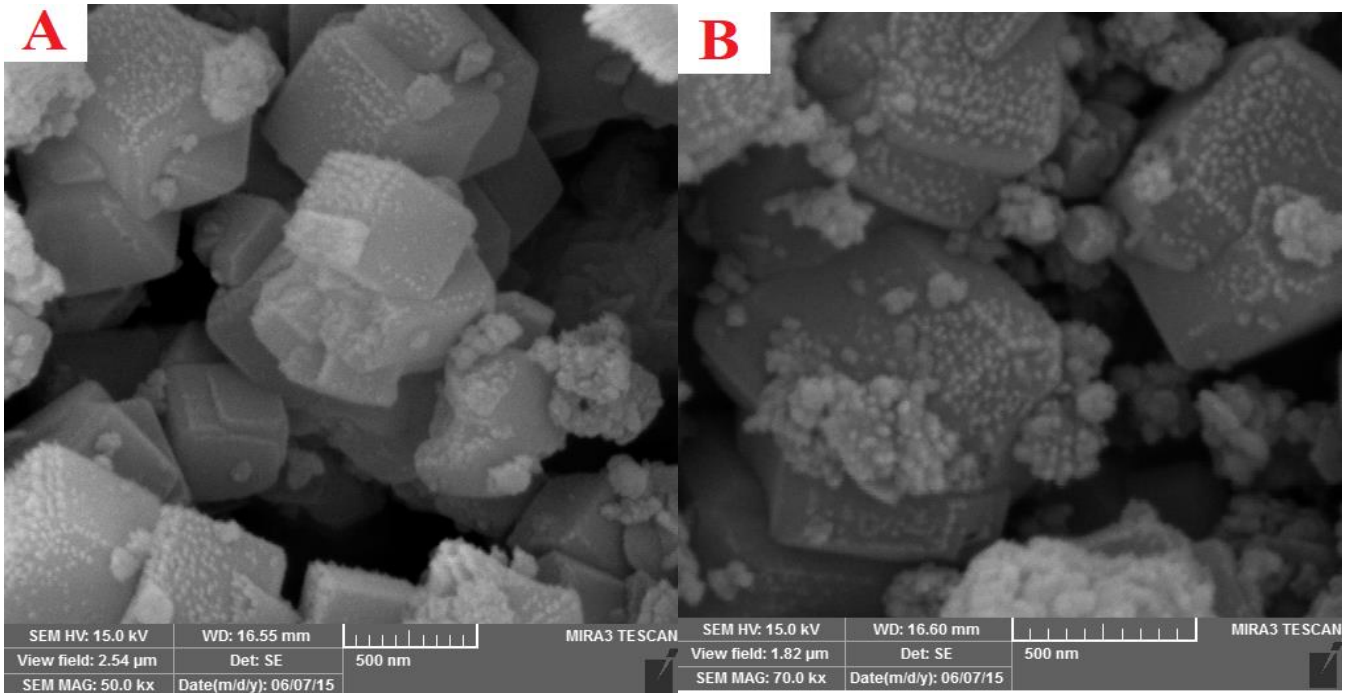


Fig. 2. SEM images of (A) IO₃NaA and (B) IO₇NaA nanocomposites along with (C) their corresponding EDX analysis

enough access to water through the pores, channels, and surface of NaA zeolite. Thus, removal efficiency decreases with the increase of Fe₃O₄ loading.

At the As(V) initial concentration of 400 g/l and adsorbent dose of 0.05 g/l, the adsorbed As(V) by IO₃NaA

zeolite reaches 83 and 87% within exposure time of 60 and 90 min, respectively. It seems that an equilibrium will be reached by increasing contact time. The percentage removal of As(V) onto the IO₃NaA zeolite versus time with different intervals (30–150 min) is represented in Fig. 4. As depicted,

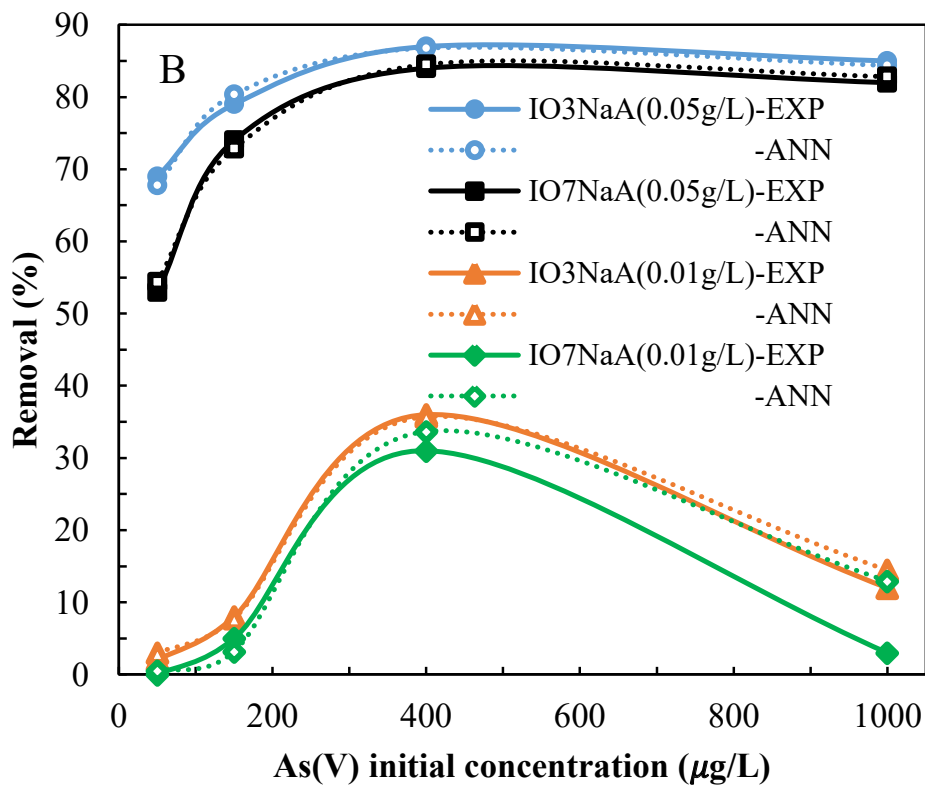
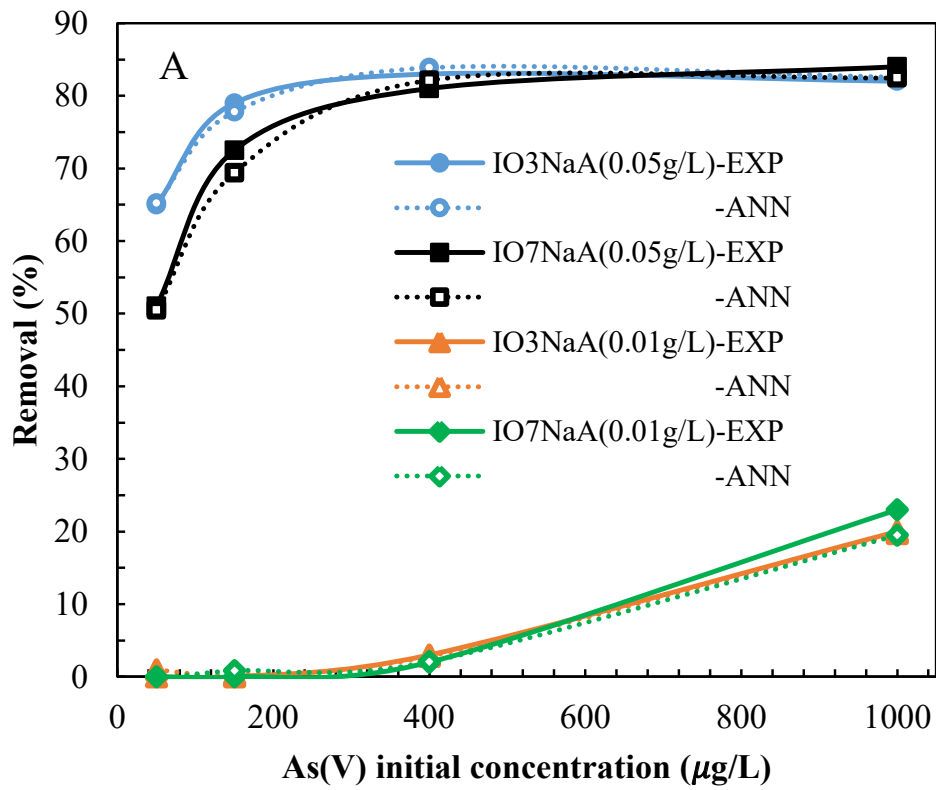


Fig. 3. Experimental (solid lines) and ANN predicted (dashed lines) values of As(V) removal by Fe3O4-

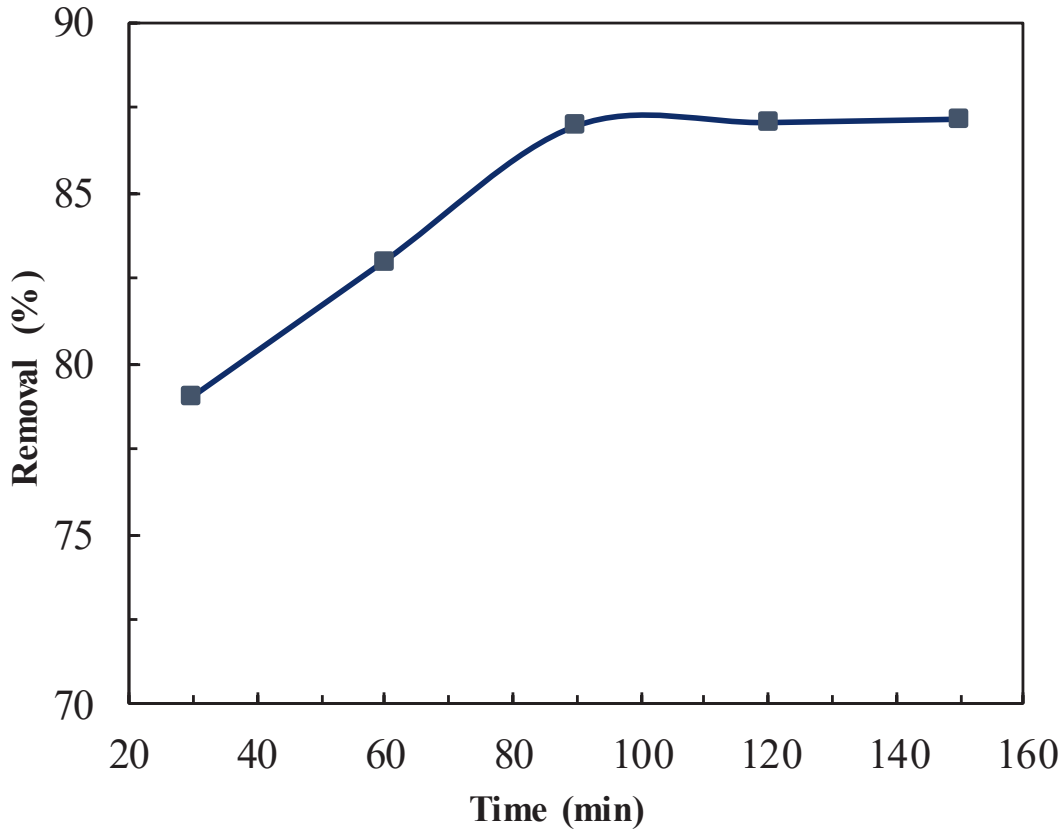


Fig. 4. Effect of contact time on the adsorption of arsenic by IO₃NaA zeolite: As(V) initial concentration 400 g/l; adsorbent dose 0.05 g/l

the removal efficiency of As(V) ions is rapid in the initial stages up to 90 min, and thereafter, is almost the same, within exposure time of 150 min. The fast adsorption rate at the initial stage could be attributed to the abundant availability of active sites on the adsorbent surface for rapid metal ions binding. However, the second stage is the slow intraparticle diffusion of metal ions into the adsorbent. A contact time of 90 min with 87% removal efficiency was considered as the equilibrium time.

3.3. Artificial Neural Network Modeling

The topology of an ANN is determined by the number of layers, the number of neurons in each layer, and the nature of transfer functions with correct identification of the set of independent input and output variables. In this work, the adsorbent dose (g/l), As(V) initial concentration (g/l), contact time (min), and percentage of Fe₃O₄ nanoparticles (%) were used as inputs of ANN model and the percentage removal of arsenic (R%) was chosen as the experimental response or output variable. Multilayer feed-forward ANN with one hidden layer was used based on the universal approximation theory which suggests that a network with a single hidden layer with a sufficiently large number of neurons can interpret any input-output structure [42]. Fig. 5(A) shows the optimized neural network structure (4-4-1), for which sigmoid transfer function in the hidden layer and a linear transfer function in

the output node was used.

It is recognized that the selection of neurons in the hidden layer is an important task when an ANN is designed. On the one hand, the convergence rate of the network may be affected by too little number of neurons. On the other hand, a large number of neurons may result in the complicated network topology, training frequency increasing, model over-fitting, and generalization reduction [31]. Therefore, the number of neurons in the hidden layer is determined according to the minimum prediction of error of the neural network in order that the error between the experimental and predicted values is minimized. To find the optimum number of neurons in the hidden layer, the network was tested with different numbers of neurons, from 1 to 10, in the hidden layer through the observation of the Mean Squared Error (*MSE*) (see Fig. 5(B)). *MSE* measures the performance of the network according to the following equation.

$$MSE = \frac{1}{N} \sum_{i=1}^N (y_{i,pred} - y_{i,exp})^2 \quad (3)$$

where N is the number of data points, $y_{i,pred}$ is the network prediction, $y_{i,exp}$ is the experimental response and i is an index of data [32].

It could be seen that the performance of the network stabilized with the inclusion of four nodes in the hidden layer.

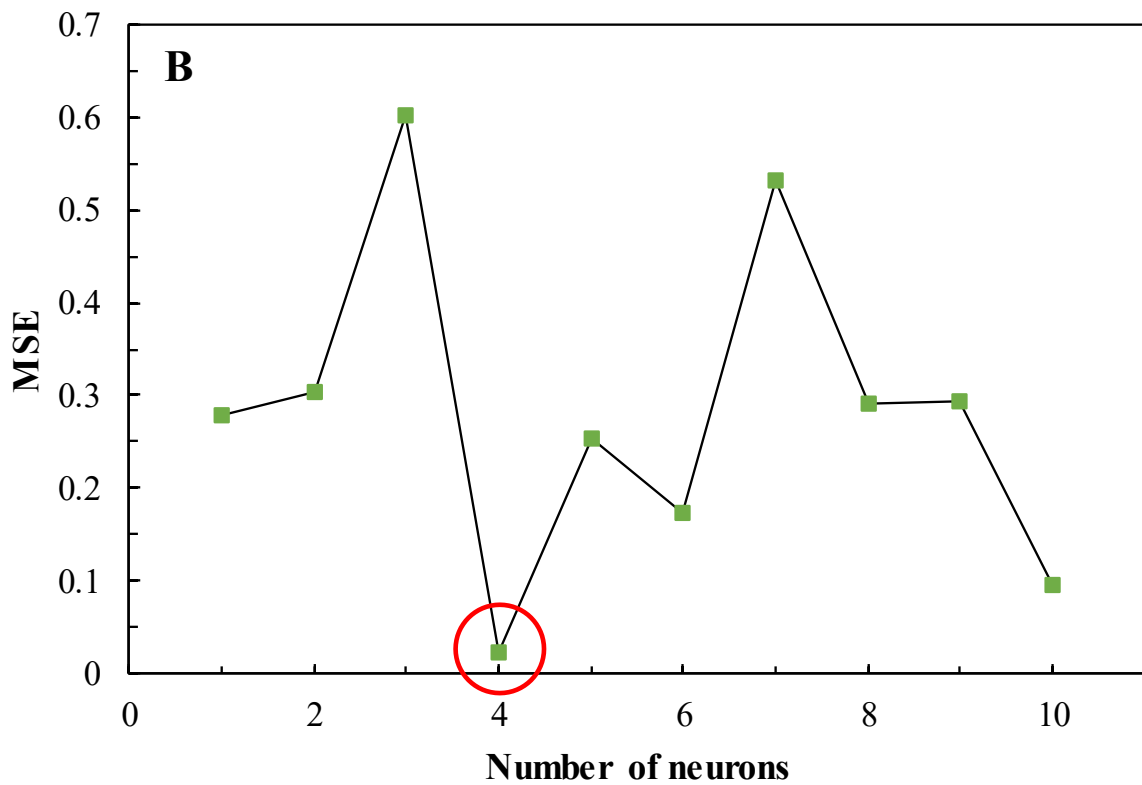
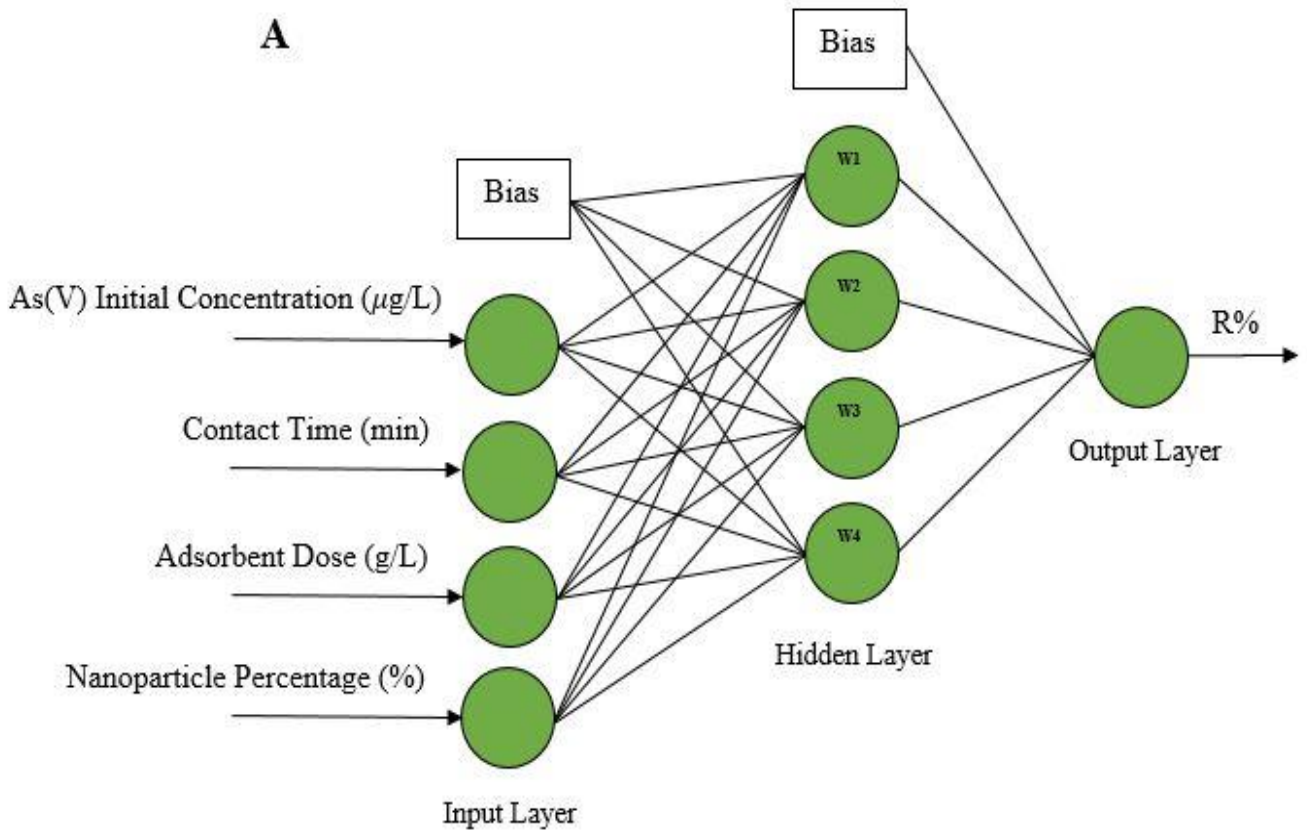


Fig. 5. (A) Pattern of optimized ANN architecture and (B) variation of MSE versus number of neurons in the hidden layer

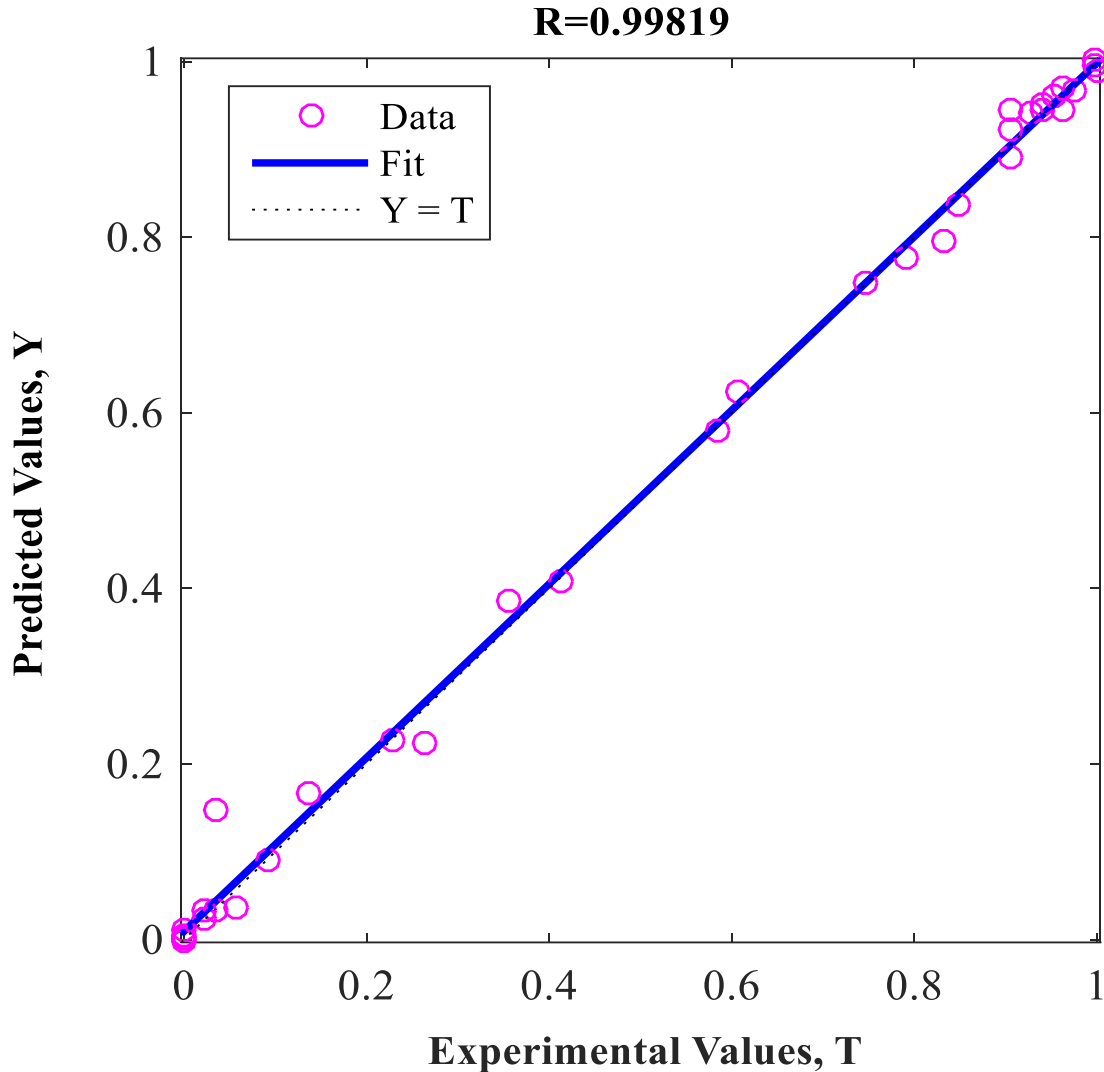


Fig. 6. Comparison of the experimental results with those calculated via neural network modeling (ANN)

So, based on the approximation of *MSE* function, a number of hidden neurons equal to four was adopted and a single layer feed forward backpropagation neural network was used for the modeling of the process. Fig. 6 shows a comparison between experimental values of the output variable ($R\%$) and predicted values using the ANN model. As seen, the points are well distributed around $Y=T$ dashed line in a narrow area. The linear fit indicated by a solid line with a correlation coefficient of $R^2=0.9981$, shows a good agreement between the predicted and experimental data. Therefore, it can be concluded that the present ANN model is suited to model the removal of As(V) from an aqueous solution by using IO_nNaA zeolites. For almost all experiments (see Fig. 3), the ANN was confirmed to be an adequate interpolation tool, where good prediction was obtained.

4. CONCLUSIONS

In the current study, Fe_3O_4 -NaA nanocomposites

(IO_nNaA) with various iron oxide contents ($n=3$ & 7 wt%) were synthesized and characterized by SEM, EDX, and XRD analyses. The synthesized Fe_3O_4 -NaA zeolite showed a high removal efficiency of As(V) from the aqueous solution. Despite the highest iron oxide content of IO_7NaA , the highest arsenic removal was obtained with the lowest iron oxide content sample (IO_3NaA). Aggregation of the nanoparticles and their inhomogeneous dispersion on the NaA zeolite surface are responsible to this situation. Under optimized conditions (percentage of Fe_3O_4 nanoparticles 3%, IO_3NaA dose 0.05 g/l, As(V) initial concentration 400 g/l and contact time 90 min), the maximum removal of arsenic was achieved as 87%. The magnetic Fe_3O_4 -NaA zeolite which can be easily separated from the medium after a magnetic process, is introduced as a kind of suitable adsorbent for removal of As(V) from aqueous solution. Artificial neural network modeling was also applied upon batch experimental values to provide the reasonable predictive performance of

the synthesized adsorbent. The findings indicated that the ANN model provides reasonable predictive performance ($R^2=0.998$) of As(V) adsorption by Fe_3O_4 -NaA. The data presented in this investigation can be further extrapolated to design and establish an efficient plan for arsenic removal from contaminated water. In fact, simulation based on the ANN model can applicably estimate the behavior of the adsorption process under different conditions, with increasing the range of experimental conditions adopted. So, investigating more affective parameters on As(V) removal by simply synthesized Fe_3O_4 -NaA zeolite such as pH, temperature and etc is proposed for conducting future research.

Acknowledgments

The authors would like to appreciate the Water and Sewage Company of East Azerbaijan Province of Iran to support the arsenic concentration tests.

REFERENCES

- [1] Y.-h. Xu, T. Nakajima, A. Ohki, Adsorption and removal of arsenic(V) from drinking water by aluminum-loaded Shirasu-zeolite, *Journal of Hazardous Materials*, 92(3) (2002) 275-287.
- [2] P. Chutia, S. Kato, T. Kojima, S. Satokawa, Arsenic adsorption from aqueous solution on synthetic zeolites, *Journal of Hazardous Materials*, 162(1) (2009) 440-447.
- [3] P. Chutia, S. Kato, T. Kojima, S. Satokawa, Adsorption of As(V) on surfactant-modified natural zeolites, *Journal of Hazardous Materials*, 162(1) (2009) 204-211.
- [4] S.R. Wickramasinghe, B. Han, J. Zimbron, Z. Shen, M.N. Karim, Arsenic removal by coagulation and filtration: comparison of groundwaters from the United States and Bangladesh, *Desalination*, 169(3) (2004) 231-244.
- [5] L.M. Camacho, R.R. Parra, S. Deng, Arsenic removal from groundwater by MnO_2 -modified natural clinoptilolite zeolite: Effects of pH and initial feed concentration, *Journal of Hazardous Materials*, 189(1) (2011) 286-293.
- [6] S. Mandal, M.K. Sahu, R.K. Patel, Adsorption studies of arsenic(III) removal from water by zirconium polyacrylamide hybrid material (ZrPACM-43), *Water Resources and Industry*, 4 (2013) 51-67.
- [7] W. Chen, R. Parette, J. Zou, F.S. Cannon, B.A. Dempsey, Arsenic removal by iron-modified activated carbon, *Water Research*, 41(9) (2007) 1851-1858.
- [8] A.I. Zouboulis, I.A. Katsoyiannis, Arsenic Removal Using Iron Oxide Loaded Alginate Beads, *Industrial & Engineering Chemistry Research*, 41(24) (2002) 6149-6155.
- [9] D. Mohan, C.U. Pittman, Arsenic removal from water/wastewater using adsorbents—A critical review, *Journal of Hazardous Materials*, 142(1) (2007) 1-53.
- [10] E.O. Kartinen, C.J. Martin, An overview of arsenic removal processes, *Desalination*, 103(1) (1995) 79-88.
- [11] M.-C. Shih, An Overview of Arsenic Removal by Pressure-Driven Membrane Processes, 172 (2005) 85-97.
- [12] M. Iwamoto, H. Kitagawa, Y. Watanabe, Highly Effective Removal of Arsenate and Arsenite Ion through Anion Exchange on Zirconium Sulfate-Surfactant Micelle Mesostructure, 31 (2002) 814.
- [13] V. Chandra, J. Park, Y. Chun, J.W. Lee, I.-C. Hwang, K.S. Kim, Water-Dispersible Magnetite-Reduced Graphene Oxide Composites for Arsenic Removal, *ACS Nano*, 4(7) (2010) 3979-3986.
- [14] Z. Zhou, Y.-g. Liu, S.-b. Liu, H.-y. Liu, G.-m. Zeng, X.-f. Tan, C.-p. Yang, Y. Ding, Z.-l. Yan, X.-x. Cai, Sorption performance and mechanisms of arsenic(V) removal by magnetic gelatin-modified biochar, *Chemical Engineering Journal*, 314 (2017) 223-231.
- [15] S.R. Kanel, B. Manning, L. Charlet, H. Choi, Removal of Arsenic(III) from Groundwater by Nanoscale Zero-Valent Iron, *Environmental Science & Technology*, 39(5) (2005) 1291-1298.
- [16] J.L. Mathieu, A.J. Gadgil, S.E. Addy, K. Kowolik, Arsenic remediation of drinking water using iron-oxide coated coal bottom ash, *J Environ Sci Health A Tox Hazard Subst Environ Eng*, 45(11) (2010) 1446-1460.
- [17] S. Lunge, S. Singh, A. Sinha, Magnetic iron oxide (Fe_3O_4) nanoparticles from tea waste for arsenic removal, *Journal of Magnetism and Magnetic Materials*, 356 (2014) 21-31.
- [18] D. Setyono, S. Valiyaveetil, Chemically Modified Sawdust as Renewable Adsorbent for Arsenic Removal from Water, *ACS Sustainable Chemistry & Engineering*, 2(12) (2014) 2722-2729.
- [19] R. Liu, L. Zhu, Z. He, H. Lan, H. Liu, J. Qu, Simultaneous removal of arsenic and fluoride by freshly-prepared aluminum hydroxide, *Colloids and Surfaces A: Physicochemical and Engineering Aspects*, 466 (2015) 147-153.
- [20] M. Šiljeg, L. Foglar, I. Gudelj, The removal of arsenic from water with natural and modified clinoptilolite, *Chemistry and Ecology*, 28(1) (2012) 75-87.
- [21] Q. Zhou, J. Wang, X. Liao, J. Xiao, H. Fan, Removal of As (III) and As (V) from water using magnetic core-shell nanomaterial Fe_3O_4 @ polyaniline, *Int J Green Technol*, 1 (2015) 55-64.
- [22] T. Stanić, A. Daković, A. Živanović, M. Tomašević-Čanović, V. Dondur, S. Milićević, Adsorption of arsenic (V) by iron (III)-modified natural zeolitic tuff, *Environmental Chemistry Letters*, 7(2) (2009) 161-166.
- [23] L. Feng, M. Cao, X. Ma, Y. Zhu, C. Hu, Superparamagnetic high-surface-area Fe_3O_4 nanoparticles as adsorbents for arsenic removal, *Journal of Hazardous Materials*, 217-218 (2012) 439-446.
- [24] Lalmunsiam, R.R. Pawar, S.-M. Hong, K.J. Jin, S.-M. Lee, Iron-oxide modified sericite alginate beads: A sustainable adsorbent for the removal of As(V) and Pb(II) from aqueous solutions, *Journal of Molecular Liquids*, 240 (2017) 497-503.
- [25] N. Gharehaghaji, B. Divband, L. Zareei, Nanoparticulate NaA zeolite composites for MRI: Effect of iron oxide content on image contrast, *Journal of Magnetism and Magnetic Materials*, 456 (2018) 136-141.
- [26] C.R. Melo, H.G. Riella, N.C. Kuhnen, E. Angioletto, A.R. Melo, A.M. Bernardin, M.R. da Rocha, L. da Silva, Synthesis of 4A zeolites from kaolin for obtaining 5A zeolites through ionic exchange for adsorption of arsenic, *Materials Science and Engineering: B*, 177(4) (2012) 345-349.
- [27] A.M. Yusof, N.A. Malek, Removal of Cr(VI) and As(V) from aqueous solutions by HDTMA-modified zeolite Y, *J Hazard Mater*, 162(2-3) (2009) 1019-1024.
- [28] Z. Yan, Z. Lin, M. Kai, M. Guozhu, The surface modification of zeolite 4A and its effect on the water-absorption capability of starch-g-poly (acrylic acid) composite, *Clays and Clay Minerals*, 62(3) (2014) 211-223.
- [29] U.K. Sahu, S. Sahu, S.S. Mahapatra, R.K. Patel, Cigarette soot activated carbon modified with Fe_3O_4 nanoparticles as an effective adsorbent for As(III) and As(V): Material preparation, characterization and adsorption mechanism study, *Journal of Molecular Liquids*, 243 (2017) 395-405.
- [30] M. Khatamian, N. Khodakarampoor, M. Saket-Oskoui, Efficient removal of arsenic using graphene-zeolite based composites, *Journal of Colloid and Interface Science*, 498 (2017) 433-441.
- [31] M. Fan, T. Li, J. Hu, R. Cao, X. Wei, X. Shi, W. Ruan, Artificial Neural Network Modeling and Genetic Algorithm Optimization for Cadmium Removal from Aqueous Solutions by Reduced Graphene Oxide-Supported Nanoscale Zero-Valent Iron (nZVI/rGO) Composites, *Materials (Basel)*, 10(5) (2017).
- [32] D. Krishna, R.P. Sree, Artificial Neural Network (ANN) Approach for Modeling Chromium (VI) Adsorption from Aqueous Solution Using a Borasus Flabellifer Coir Powder, *International Journal of Applied Science and Engineering*, 12(3) (2014) 177-192.

- [33] A. Kardam, K.R. Raj, J.K. Arora, M.M. Srivastava, S. Srivastava, Artificial Neural Network Modeling for Sorption of Cadmium from Aqueous System by Shelled Moringa Oleifera Seed Powder as an Agricultural Waste, *Journal of Water Resource and Protection*, Vol.02No.04 (2010) 339-344.
- [34] B. Singha, N. Bar, S.K. Das, The use of artificial neural networks (ANN) for modeling of adsorption of Cr(VI) ions, *Desalination and Water Treatment*, 52(1-3) (2014) 415-425.
- [35] H. Esfandian, M. Parvini, B. Khoshandam, A. Samadi-Maybodi, Artificial neural network (ANN) technique for modeling the mercury adsorption from aqueous solution using Sargassum Bevanom algae, *Desalination and Water Treatment*, 57(37) (2016) 17206-17219.
- [36] S. Zavareh, Z. Farrokhzad, F. Darvishi, Modification of zeolite 4A for use as an adsorbent for glyphosate and as an antibacterial agent for water, *Ecotoxicol Environ Saf.*, 155 (2018) 1-8.
- [37] W.-M. Xie, F.-P. Zhou, X.-L. Bi, D.-D. Chen, J. Li, S.-Y. Sun, J.-Y. Liu, X.-Q. Chen, Accelerated crystallization of magnetic 4A-zeolite synthesized from red mud for application in removal of mixed heavy metal ions, *Journal of Hazardous Materials*, 358 (2018) 441-449.
- [38] A.R. Loiola, J.C.R.A. Andrade, J.M. Sasaki, L.R.D. da Silva, Structural analysis of zeolite NaA synthesized by a cost-effective hydrothermal method using kaolin and its use as water softener, *Journal of Colloid and Interface Science*, 367(1) (2012) 34-39.
- [39] T. Qian, J. Li, Synthesis of Na-A zeolite from coal gangue with the in-situ crystallization technique, *Advanced Powder Technology*, 26(1) (2015) 98-104.
- [40] A. Shoumkova, V. Stoyanova, SEM-EDX and XRD characterization of zeolite NaA, synthesized from rice husk and aluminium scrap by different procedures for preparation of the initial hydrogel, *Journal of Porous Materials*, 20(1) (2013) 249-255.
- [41] X. Zhang, D. Tang, G. Jiang, Synthesis of zeolite NaA at room temperature: The effect of synthesis parameters on crystal size and its size distribution, *Advanced Powder Technology*, 24(3) (2013) 689-696.
- [42] A. Khataee, A. Khani, Modeling of Nitrate Adsorption on Granular Activated Carbon (GAC) using Artificial Neural Network (ANN), in: *International Journal of Chemical Reactor Engineering*, (2009).
- [43] M.V. Nagarpita, P. Roy, S.B. Shruithi, R.R.N. Sailaja, Synthesis and swelling characteristics of chitosan and CMC grafted sodium acrylate-co-acrylamide using modified nanoclay and examining its efficacy for removal of dyes, *Int J Biol Macromol*, 102 (2017) 1226-1240.

HOW TO CITE THIS ARTICLE

L. Sanaei, M. Tahmasebpour, M. Khatamian, B. Divband, *Arsenic Removal from Aqueous Solutions using Iron Oxide-modified Zeolite: Experimental and Modeling Investigations*, *AUT J. Mech. Eng.*, 5(1) (2021) 141-152.

DOI: [10.22060/ajme.2020.17214.5849](https://doi.org/10.22060/ajme.2020.17214.5849)



